Active and Reactive Power Sharing Between Three-Phase Winding Sets of a Multiphase Induction Machine

I. Subotic, *Member, IEEE,* O. Dordevic, *Member, IEEE,* J. B. Gomm, *Member, IEEE,* E. Levi, *Fellow, IEEE*

***Abstract*—This paper introduces a method which can accurately transfer active and reactive power between sets of three-phase windings of a multiphase induction machine (IM). The machine has to have a multiple of three phases (3, 6, 9 etc.), with each three phases representing one set. The paper demonstrates first that the sets do not share the power in the same way as they share a torque. Therefore, the paper proposes a method that is capable of achieving accurate power sharing. This is ensured by considering the whole power that is transferred through the air-gap to/from a set, instead of considering only a power that is transferred between that set and a rotor shaft. A complete control algorithm of the proposed method is given. Experiments and simulations verify theoretical considerations and the proposed control.**

***Index Terms*-- Bidirectional power flow, induction motors, inductive power transfer, microgrids, active power control, reactive power control, smart grids, wind power generation.**

I. Introduction

A concept of connecting electrical terminals of a single machine to multiple energy sources/consumers simultaneously (Fig. 1) recently became of interest. The machine has to have multiple sets of three phases (3, 6, 9, etc. phases), which can be connected to different energy sources/sinks (Fig. 2). A restriction is that a three-phase set cannot be connected to more than one energy source/sink. The main motivation behind this topology is that the energy sources/sinks can exchange the power between them through the machine, but without interfering with its (machine's) mechanical operation (Fig. 3).

A demand for such a concept came from two emerging applications. The first application are microgrids. They are small-scale power systems that can generate, distribute and regulate a power flow to local consumers [1]. They are capable of operating in islanding mode, and can be of ac [2] or dc [3] type. With the concept elaborated above it is possible to connect the same wind turbine to multiple isolated microgrids, as in Fig. 1. This provides the benefit of allowing bidirectional power flow between the microgrids while retaining galvanic isolation.

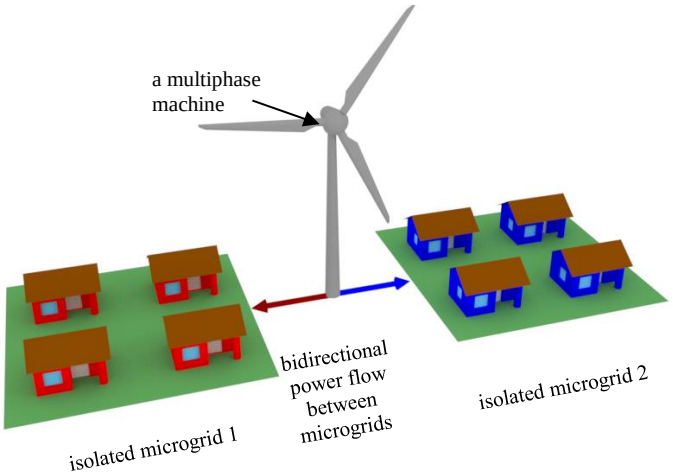

Fig. 1. A single multiphase machine can be used for power transfer from one microgrid to another. The microgrids are mutually isolated.

The second application are electric vehicles (EVs) supplied from multiple energy sources [4]. The benefit remains the same: allowing arbitrary power flow direction between the energy sources through the machine, while not interfering with the normal vehicle propulsion mode of operation.

The concept was successfully applied to permanent magnet (PM) machines, with the validity demonstrated on a six-phase [5] and a nine-phase machine [6], [7]. The approach was further found to be very useful in devising regenerative testing methods for machines with multiple three-phase windings, as detailed for twelve- and six-phase PM machines in [8], [9] and [10], respectively. The concept was also tested on multiphase induction machines (IMs). Ability of different sets of windings to produce different amounts of torque was demonstrated for a dual (double) three-phase [11], a six-phase [12]-[14], a nine-phase [15], and a twelve-phase machine [16]-[18].

This paper provides the following contributions:

i) A demonstration that, if IMs are employed, the sets of three-phase windings do not share power in the same way as they share a torque.
ii) It proposes a method that can achieve accurate active and reactive power transfer between winding sets of an IM.
iii) In case where only active power transfer is of interest, it proposes optimal control of reactive power, which minimizes additional stator winding losses of the IM, caused by the power sharing.

Manuscript received June 26, 2018; revised December 11, 2018; accepted February 02, 2019.

The authors acknowledge the Engineering and Physical Sciences Research Council (EPSRC), U.K., for supporting the 'Power flow control in future electric vehicles and dc microgrids with multiple energy sources' project (EP/P00914X/1).

I. Subotic, O. Dordevic, J. B. Gomm and E. Levi are with the Faculty of Engineering and Technology, Liverpool John Moores University, Liverpool L3 3AF, U.K. (e-mail: ivansubotic86@gmail.com; o.dordevic@ljmu.ac.uk; j.b.gomm@ljmu.ac.uk; e.levi@ljmu.ac.uk).

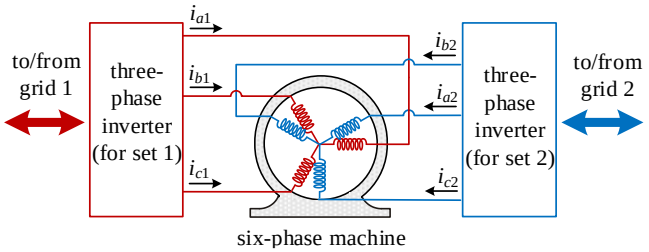

Fig. 2. Winding sets of a multiphase machine are connected to different isolated energy sources/sinks through inverters. A six-phase case is shown.

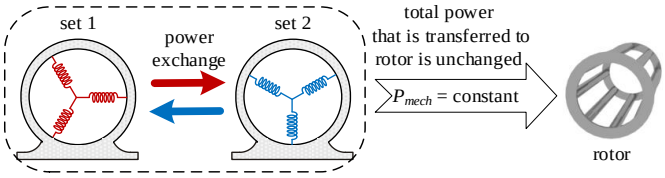

Fig. 3. Sets can exchange power between them without affecting the rotor. The total, combined, influence of all sets on the rotor remains the same.

Application of the here proposed power sharing algorithm to different control and machine types is believed to be possible but is beyond the scope of this manuscript.

The paper is organised as follows. Section II elaborates a basic principle of operation that is valid for both torque and power sharing. A theoretical comparison between torque and power sharing is provided in Section III. Sections IV and V provide a complete control algorithm. Verification of the theoretical results by experiments and simulations is provided in Section VI. Section VII concludes the paper.

II. Basic Principle of Operation

One way of observing machines with multiple sets of three-phase windings is by utilizing a so-called "multi-stator" (also called "multi-*dq*" or "multi three-phase") approach [19]. This method is popular because it allows basic understanding of multiphase machines by employing well-known knowledge of three-phase machines. Without any loss of generality, a machine with two three-phase sets is considered further on.

An attempt to graphically represent the "multi-stator" approach is provided in Fig. 4. The number of "stators" matches the number of winding sets of the machine. Each "stator" produces a certain amount of flux in the rotor. The total flux that originates from all stators and enters the rotor is a sum of their individual contributions (Fig. 4). This flux does not include influence of rotor bars. Therefore, it should not be confused with the total flux in the rotor (which includes the flux production of the rotor bars) and which is commonly called "rotor flux".

From a rotor's perspective, it does not matter whether the total flux that originates from all stators comes from multiple stators or a single stator. It only experiences their sum. Thus, by controlling the sum, the machine can be controlled in the same manner as two three-phase machines.

On the other hand, individual contribution of each "stator" to that sum is not of importance from a perspective of torque production (as long as the sum is the same). This introduces a degree of freedom that does not influence torque (although it affects total losses; thus care should be taken in order to avoid

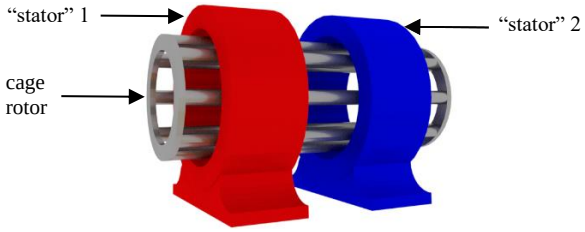

Fig. 4. A graphical representation of the "multi-stator" approach. Although the "stators" belong to the same machine, they are shown as physically separated. Both "stators" produce flux through bars of the same rotor.

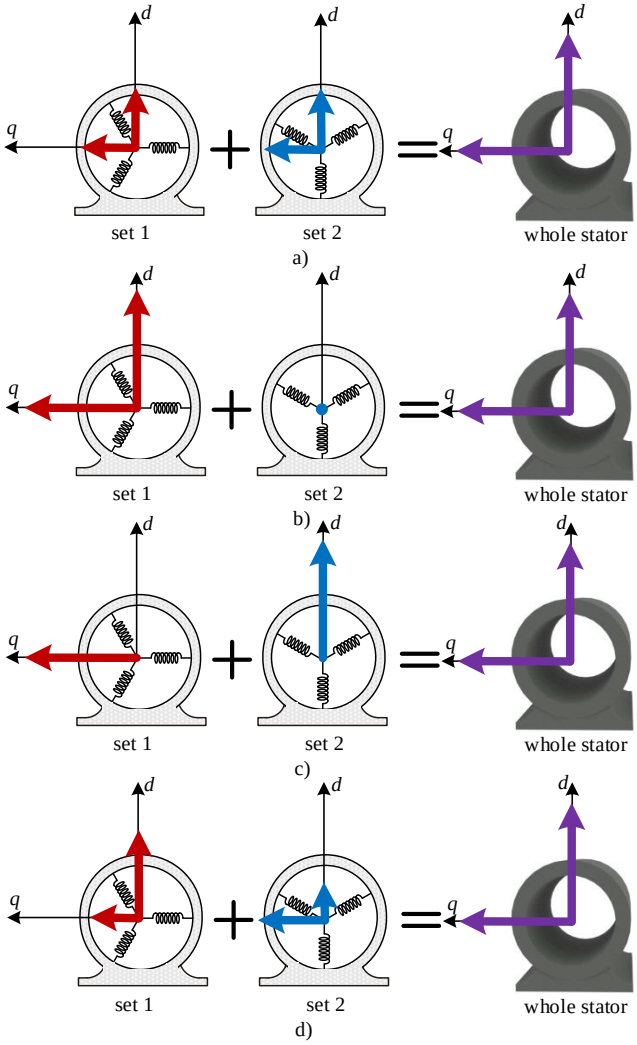

Fig. 5. Various manners of forming the same total flux that originates from stator (coloured in purple): a) both sets have equal contributions; b) set 1 produces the whole flux; c) set 1 produces the flux in *q*-axis (red), while set 2 gives flux in *d*-axis (blue); d) a general case in which both sets produce flux in both axes.

overheating of the machine). This is illustrated in Fig. 5. The two sets ("stators") from Fig. 5 have variable individual contributions, while their sum is always the same. It is clear that in Fig. 5a the sets produce equal amounts of torque, while in Fig. 5b all the torque (and power) comes just from the first set. This mode is particularly useful for enabling a fault-tolerant operation [16]. A general case is shown in Fig. 5d. Rotor torque is always fixed. Thus, power is effectively transferred from one set (stator) to another (Fig. 3) by utilizing the additional degrees of freedom.

While in the general case (Fig. 5d) it is clear that power is transferred from one set to another, its exact amount is not obvious. This is discussed in the next section.

III. Theoretical Considerations

Three powers are of interest for the following theoretical considerations. The first is electrical power of a set (or of a phase). It refers to powers on its terminals. If phase "*a*" and set 1 (which consists of e.g. three phases) are observed, the electrical powers of a phase P_{a1} (Fig. 6a) and a set P_1 (Fig. 6b) can be expressed as:

$$P_{a1} = V_{a1} \cdot I_{a1} \cos(\measuredangle v_{a1} - \measuredangle i_{a1}); \quad P_1 = 3 \cdot P_{a1}\,, \tag{1}$$

where V_{a1} and I_{a1} are fundamental RMS values of phase voltage and current of phase a_1 (i.e. v_{a1} and i_{a1}), and the set has balanced currents. Phase a_1 stands for a phase "*a*" of the set 1.

The second power of interest is a power that is transferred to/from a set (or a phase) through the air-gap. If again phase "*a*" and set 1 are observed, the transferred powers of a phase (P_{Ta1}) and a set (P_{T1}) can be written as:

$$P_{Ta1} = E_{a1\_gap} \cdot I_{a1} \cos(\measuredangle e_{a1_{gap}} - \measuredangle i_{a1});\; P_{T1} = 3 \cdot P_{Ta1}\,, \tag{2}$$

where E_{a1_gap} is fundamental's RMS value of e_{a1_gap}. The variable e_{a1_gap} is back-EMF (electro-motive force) that is induced in the phase a_1 by air-gap flux Φ_{gap}. It is governed by:

$$e_{a1\_gap} = \frac{\mathrm{d}(N_{\mathrm{turns}} \cdot \Phi_{\mathrm{gap}})}{\mathrm{d}t}, \tag{3}$$

where N_{turns} is the number of turns of the phase a_1. From measurable currents and voltages, this back-EMF is obtained,

$$e_{a1\_gap} = v_{a1} - R_s i_{a1} - L_{\gamma s} \frac{\mathrm{d}i_{a1}}{\mathrm{d}t}, \tag{4}$$

where R_s and $L_{\gamma s}$ are stator phase resistance and leakage inductance, respectively.

Finally, the third power of interest is the power that is transferred from a set to a rotor shaft. This is mechanical power. For the set 1 it is annotated as $P_{\mathrm{mech\_1}}$ and defined as:

$$P_{\mathrm{mech\_1}} = T_1 \cdot \Omega \sim \Phi_r \cdot i_{q1} \cdot \Omega, \tag{5}$$

where T_1 is a torque produced by the set 1 (Fig. 6b), Ω mechanical speed, Φ_r rotor flux and i_{q1} the first set's current component that is perpendicular to the rotor flux Φ_r.

From (2)-(3) it can be seen that P_{T1} is governed by the air-gap flux Φ_{gap}. On the other hand, from (5) it is obvious that P_{mech_1} is governed by rotor flux Φ_r. These two fluxes are different. In order to facilitate their understanding, they are illustrated in Figs. 7 and 8.

Fig. 7 shows how the rotor flux Φ_r is formed from two contributing fluxes. The first is the total flux (shown in the right-hand part of Fig. 5) that comes from all sets (stators) and enters the rotor. The second is a flux that is produced by rotor bars. Formation of the air-gap flux Φ_{gap} is shown in Fig. 8. As is well-known, it is obtained from rotor flux by subtracting rotor leakage flux. Hence the rotor flux Φ_r and the air-gap flux Φ_{gap} have different directions and amplitudes.

A. Torque Sharing

As follows from (5), a torque T_n, that is produced by a set, depends on rotor flux Φ_r. If this flux is kept constant, the torque is only dependant on the set's current component that is perpendicular to this flux, as indicated in (5). In a coordinate system which is oriented according to it (Φ_r), this is set's current on q-axis. Therefore, if a sum of the q-axis components of the currents from individual sets is kept constant,

$$i_{q1} + i_{q2} = i_q = \mathrm{const}, \tag{6}$$

it is possible to achieve different torque contributions (to total torque) from different sets without interfering with machine's operation. Clearly, the sets share the torque according to their q-current components.

Practical implication is the following. If there are e.g. two winding sets in the machine and one set should produce e.g. three times higher torque than the other, the only thing that has to be done is to set q-current of that set to be three times higher than the q-current of the other (and make sure that the total i_q is unchanged). This concept is well covered in literature [11]-[18].

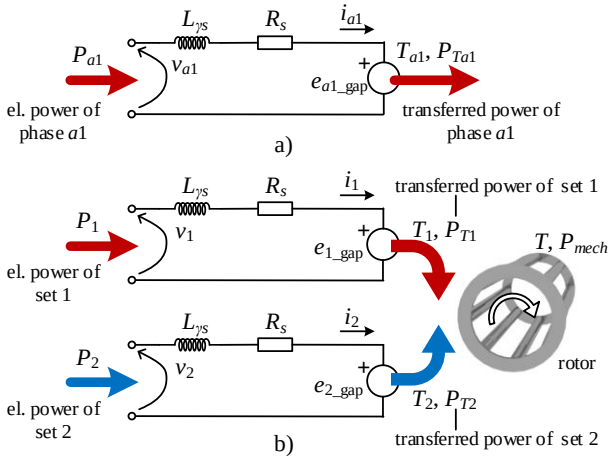

Fig. 6. Demonstration of electrical power, transferred power and torque that are produced by: a) single phase, b) each set of windings. P_n is electrical power of a set n, P_{Tn} is transferred power from the set n, T_n is a torque that is produced by set n. T stands for total torque and P_{mech} for total mechanical power.

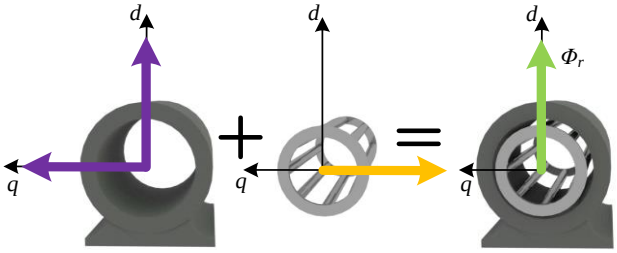

Fig. 7. Formation of rotor flux (green) from two contributing fluxes. The first is total flux that is produced by all stator sets (purple). The second is a flux that is produced by rotor bars (yellow).

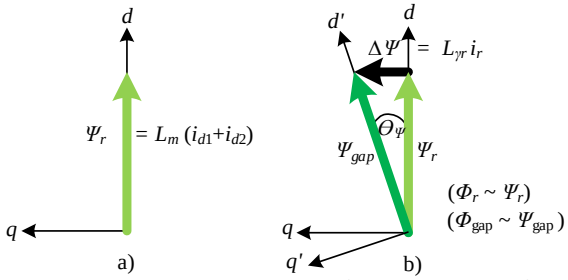

Fig. 8. Graphical comparison between rotor flux (a) and air-gap flux (b). Ψ_r and Ψ_{gap} are rotor flux linkage and air-gap flux linkage, respectively.

B. Power Sharing

From (2)-(3) it follows that transferred active power to/from a set is dependant on air-gap flux Φ_{gap}. If this flux is kept constant, the transferred active power to/from a set depends only on set's current component that is perpendicular to the air-gap flux. If a coordinate system is oriented according to the air-gap flux Φ_{gap}, this is a component that lays on horizontal axis, which is further annotated as q' axis (Fig. 8b).

Therefore, if a sum of q'-axis components of currents from individual sets is kept constant,

$$i_{q'1} + i_{q'2} = i_{q'} = \text{const}, \tag{7}$$

it is possible to achieve different transferred active powers from different sets without interfering with machine's operation. This has the effect as transferring active power from one set to another (Fig. 3).

The same can be concluded for a relationship between current component on d'-axis (aligned with Φ_{gap}, Fig. 8b) and transferred reactive power to/from a set.

Practical implication is the following. If there are e.g. two sets in the machine and one set should produce e.g. three times more active power than the other, the only thing that has to be done is to set q'-current of that set to be three times higher than the q'-current of the other (and make sure that the total $i_{q'}$ is unchanged). This concept is not covered in literature.

It is clear that d' current component of a set does not affect active power transfer. Similarly, q' current component does not affect reactive power transfer. On the other hand, rotor flux Φ_r and air-gap flux Φ_{gap} have different directions (Fig. 8). This means that the active power, transferred to/from a set, depends on both d- and q-axis current component of a set. Therefore, the sets do not share the power in the same way they share a torque.

C. Minimization of Additional Power Sharing Caused Losses

If only active power sharing is of interest, there exists an additional degree of freedom (namely sets' currents along d'-axis) which controls reactive power sharing. This degree of freedom can be utilized in a very simple manner to ensure minimal additional stator copper losses, introduced by uneven power sharing (which has only a minor influence on iron losses). Space vector of a set current can be written as

$$\underline{i}_{d'q'1} = i_{d'1} + j \cdot i_{q'1}. \tag{8}$$

Using power invariant transformation, copper losses that are produced by a set are

$$P_{1cu} = R_s \cdot i_{d'1}^2 + R_s \cdot i_{q'1}^2. \tag{9}$$

Total stator copper losses are

$$P_{cu} = R_s \cdot \left(i_{d'1}^2 + \cdots + i_{d'N}^2\right) + R_s \cdot \left(i_{q'1}^2 + \cdots + i_{q'N}^2\right), \tag{10}$$

where N is a number of sets in the IM.

The second term of (10) is already defined by active power sharing requirements. The first term of (10) should be minimized while ensuring that the total $i_{d'}$ does not change.

It is beneficial to express each d'-current of a set by showing how much it differs from an average value of d'-currents (i.e. $i_{d'1} = (i_{d'}/N) * (1 + a)$, where a is the difference). Therefore, the d'-currents can be represented as

$$[i_{d'1}, i_{d'2}, \ldots, i_{d'N}] = \frac{i_{d'}}{N} \cdot (1 + [a, b, \ldots, m]), \tag{11}$$

where $[a, b, \ldots, m]$ are degrees of freedom, and their sum has to be zero, in order to have total d'-current component unchanged. By applying (11) to the first term of (10), one gets

$$R_s(i_{d'1}^2 + \ \ldots + i_{d'N}^2) = R_s\left(\frac{i_{d'}}{N}\right)^2 \cdot (N + a^2 + \cdots + m^2). \tag{12}$$

Clearly, (12) becomes minimal for

$$a^2 + b^2 + \cdots + m^2 = 0 \ \ \Longrightarrow \ \ a = b = \cdots = m = 0. \tag{13}$$

It can be concluded that, in order to minimize stator copper losses, reactive powers of individual sets should always be the same, regardless of the active power sharing.

IV. The Main Control Algorithm

The multiphase machine is operated by the rotor field oriented control (RFOC) algorithm that is shown in Fig. 9. The "power sharing" block does not affect mechanical behaviour of the IM. This block is covered in detail in Section V. Without this block the control algorithm from Fig. 9 becomes the standard RFOC algorithm for multiphase machines [20].

From Fig. 9 it can be seen that RFOC algorithms for multiphase and three-phase IMs are similar. However, there are three differences.

The first difference is in the blocks "decoup. transf." and "rotat. transf.", which stand for decoupling and rotational transformation. Since the machine has more than three phases, these transformations have to transform more than three components. The additional components appear with a suffix xy in Fig 9. The general decoupling (i.e. vector space decomposition – VSD) transformation for multiphase machines can be found in [20], and is given with:

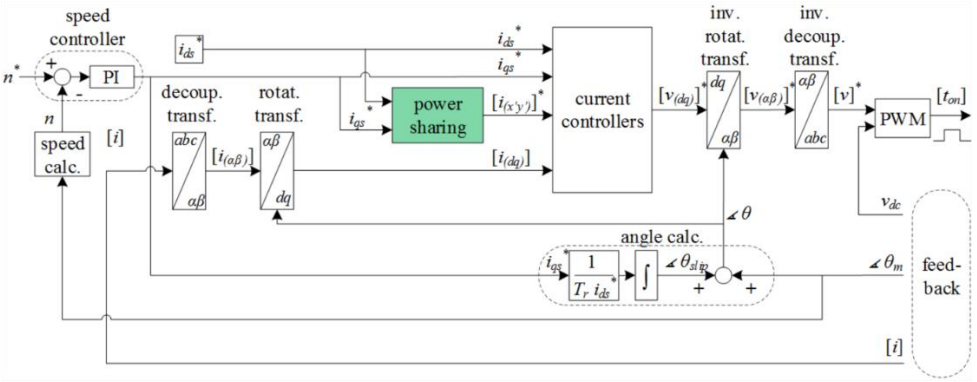

Fig. 9. Rotor field oriented control (RFOC) algorithm of multiphase IMs. Power sharing block (coloured in green) allows power sharing between sets of windings of the IM and it presents the only difference from the standard RFOC for multiphase IMs.

$$C_{ph} = \sqrt{\frac{2}{ph}} \begin{matrix} \alpha \\ \beta \\ x_1 \\ y_1 \\ \vdots \\ 0_1 \\ 0_2 \end{matrix} \begin{bmatrix} 1 & \cos(\alpha) & \cos(2\alpha) & \dots & \cos(\alpha) \\ 0 & \sin(\alpha) & \sin(2\alpha) & \dots & -\sin(\alpha) \\ 1 & \cos(2\alpha) & \cos(4\alpha) & \dots & \cos(2\alpha) \\ 0 & \sin(2\alpha) & \sin(4\alpha) & \dots & -\sin(2\alpha) \\ \vdots & \vdots & \vdots & \ddots & \vdots \\ 1/\sqrt{2} & 1/\sqrt{2} & 1/\sqrt{2} & \dots & 1/\sqrt{2} \\ 1/\sqrt{2} & -1/\sqrt{2} & 1/\sqrt{2} & \dots & -1/\sqrt{2} \end{bmatrix} \quad (14)$$

where $\alpha = 2\pi/ph$ and ph is the total number of phases. Depending on the number of isolated neutral points, and whether the machine is asymmetrical or symmetrical, C can have slightly different forms than (14), which are omitted.

There are also additional (xy) components that enter into rotational transformation block, which transforms pairs of additional inputs into a reference frame that rotates at a synchronous speed. However, it transforms each second additional input pair (x_2y_2, x_4y_4, etc.) into synchronous direction (the same direction as for the $\alpha\beta$ components), and all other input pairs (x_1y_1, x_3y_3, etc.) into a reference frame that rotates in the opposite direction.

The second difference appears in the "current control" block. The difference is caused by the additional components that are formed by the decoupling transformation block and which also have to be controlled. Thus, additional current controllers are required for controlling them (Fig. 10). When there is no need for specific torque or power sharing, references for these additional components are set to zero.

The third, and final, difference is in the PWM block. It also has more than three inputs. Zero sequence injection has to have a different form and it has to be applied to each set separately [21].

V. Control Algorithm For Torque and Power Sharing

A. Torque Sharing

The "power sharing" block from Fig. 9 is shown separately in Fig. 11. It can be seen that it consists of two blocks. The block "coeffs. correction" is only utilized if power sharing is required. This block is covered in the next subsection (which is dedicated to power sharing). Thus, only the "torque sharing" block is elaborated here.

The "torque sharing" block from Fig. 11 is shown in Fig. 12. Its operating principle is already known in literature [15]. Desired sets' torques can be expressed in the matrix form as

$$[T_1^*, T_2^*, \dots, T_N^*] = \frac{[k_1, k_2, \dots, k_N]}{k_1 + \dots + k_N} \cdot T^*, \quad (15)$$

where k_1, k_2,…,k_N are torque sharing coefficients. According to Section III-*A* (which in effect states that $i_{q1}^*: i_{q2}^*: \dots : i_{qN}^* = T_1^*: T_2^*: \dots : T_N^*$), in order to achieve torque sharing, references for q current components should be set to

$$[i_{q1}^*, i_{q2}^*, \dots, i_{qN}^*] = \frac{[k_1, k_2, \dots, k_N]}{k_1 + \dots + k_N} \cdot i_q^*. \quad (16)$$

From Fig. 12 it can be seen that the input references are given as total dq currents (i_d^* and i_q^*) and torque sharing coefficients (k_{d123} and k_{q123}). These are transformed into another set of references (in the first block of Fig. 12), which are called "multi-stator" references (i_{d123}^* and i_{q123}^*). They allow easier control of individual sets of IM. A domain in which it is possible to control all the sets (and phases) of the IM and still to keep good transient performance is VSD domain. Therefore, in this paper, the references are transformed from the "multi-stator" to VSD domain in the second block of Fig. 12.

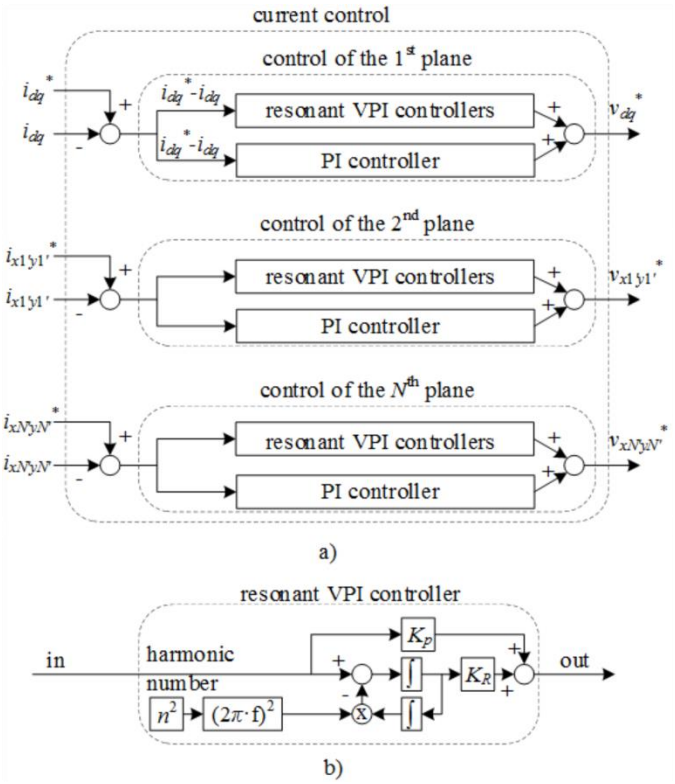

Fig. 10. a) "Current controllers" block from Fig. 9, b) "resonant vector proportional integral (VPI) controller" block from Fig. 10a.

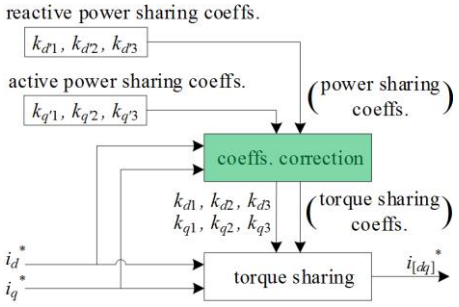

Fig. 11. "Power sharing" block from Fig. 9 (a nine-phase IM is assumed, so that there are three coefficients). The block "coeffs. correction" is the only difference from the standard torque sharing algorithm (e.g. [15]).

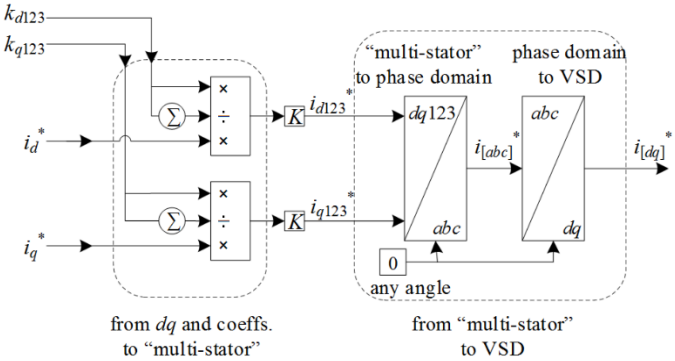

Fig. 12. "Torque sharing" block from Fig. 11. The gain K is 1 if amplitude invariant decoupling transformation is used. A nine-phase IM is assumed.

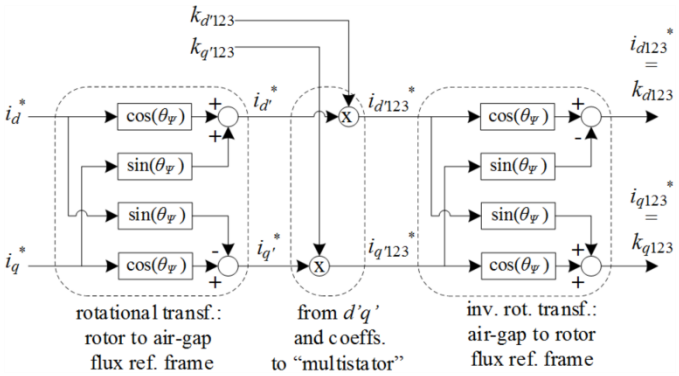

Fig. 13. "Coeffs. correction" block from Fig. 11.

B. Power Sharing

As it is demonstrated in Section III-*B*, the sets share reactive/active power through the *d*'/*q*' axes that are parallel/perpendicular to the air-gap flux Φ_{gap}. Desired transferred powers of the sets can be expressed in matrix form,

$$[P^*_{T1}, P^*_{T2}, \dots, P^*_{TN}] = \frac{[k_{q'1}, k_{q'2}, \dots, k_{q'N}]}{k_{q'1}+\dots+k_{q'N}} \cdot P^*_T,$$

$$[Q^*_{T1}, Q^*_{T2}, \dots, Q^*_{TN}] = \frac{[k_{d'1}, k_{d'2}, \dots, k_{d'N}]}{k_{d'1}+\dots+k_{d'N}} \cdot Q^*_T, \quad (17)$$

where $k_{q'1}$, $k_{q'2}$,…, $k_{q'N}$ and $k_{d'1}$, $k_{d'2}$,…, $k_{d'N}$ are active and reactive power sharing coefficients, respectively. According to Section III-*B*, in order to achieve power sharing, references for *q'* and *d*' current components should be set to

$$[i^*_{q'1}, i^*_{q'2}, \dots, i^*_{q'N}] = \frac{[k_{q'1}, k_{q'2}, \dots, k_{q'N}]}{k_{q'1}+\dots+k_{q'N}} \cdot i^*_{q'},$$

$$[i^*_{d'1}, i^*_{d'2}, \dots, i^*_{d'N}] = \frac{[k_{d'1}, k_{d'2}, \dots, k_{d'N}]}{k_{d'1}+\dots+k_{d'N}} \cdot i^*_{d'}. \quad (18)$$

On the other hand, the sets share the torque through axis that is perpendicular to rotor flux Φ_r (Section III-*A*). Also, the RFOC (Fig. 9) is implemented in this (rotor flux, Φ_r, oriented) reference frame. Naturally, it is beneficial to control all the quantities in the same reference frame. Therefore, the power sharing coefficients have to be transferred from one reference frame to another. This adjustment is done in the "coeffs. correction" block (Fig. 11), which represents the main advance, provided by the paper. It is shown separately in Fig. 13. The block provides correlation between power and torque sharing coefficients by using the following relationship between *dq* and *d'q'* current references:

$$\begin{bmatrix} i^*_d \\ i^*_q \end{bmatrix} = \begin{bmatrix} \cos(\theta_\Psi) & -\sin(\theta_\Psi) \\ \sin(\theta_\Psi) & \cos(\theta_\Psi) \end{bmatrix} \cdot \begin{bmatrix} i^*_{d'} \\ i^*_{q'} \end{bmatrix}, \quad (19)$$

where θ_Ψ is the angle between the air-gap flux Φ_{gap} and the rotor flux Φ_r. It can be obtained purely from Fig. 8 as

$$\theta_\Psi = \arctan\frac{i^*_r \cdot L_{\gamma r}}{\Psi^*_r} = \arctan\frac{(i^*_q \frac{L_m}{L_m+L_{\gamma r}})L_{\gamma r}}{i^*_d \cdot L_m}. \quad (20)$$

The finally obtained current references $i_{d123}{}^*$ and $i_{q123}{}^*$ can be used as torque sharing coefficients (only their ratio matters).

C. Minimization of Additional Stator Winding Losses

As it is shown in Section III-*C*, minimization of stator copper losses occurs when *d'* current components of all sets are equal to each other. Therefore, it can be ensured by setting

$$i^*_{d'1} = i^*_{d'2} = \dots = i^*_{d'N} = \frac{i^*_{d'}}{N}, \quad (21)$$

regardless of active power sharing.

VI. Experimental Results

Experiments are performed in order to verify theoretical results of Section III and control from Sections IV and V. The experimental rig and the connection diagram are shown in Fig. 14. A dc voltage of 600 V is provided by a linear amplifier "Spitzenberger & Spies". It supplies two custom-made converters sharing a dc link and operating at 5 kHz. A nine-phase IM is mechanically coupled with a dc machine, which is loaded with a variable resistor at its armature terminals. The rig data are given in the Appendix. Gains of the current controllers are set manually, using trial-and-error.

A. Torque Sharing

The nine-phase IM is controlled at the constant speed of 1000 rpm while it is loaded with its rated torque (7 Nm). Torque references for different sets are set to vary in time and they are given in the left part of Table I (0-1s), sectors **1**-**4**.

Currents and phase voltages of phases a_1, a_2 and a_3 (the first phase of each set) are measured by two oscilloscopes with the same external trigger. Transferred active powers (that are sent from each set into the air-gap) are then obtained from (4) and (2). Transferred reactive powers are obtained in a similar manner. The experimental results are given in the left part of Fig. 15 (0-1s, sectors **1**-**4**), while simulation results are given in the left part of Fig. 16 (0-1s). In order to reduce noise, an *RC* filter (f_c = 50Hz) is applied to dc signals.

For this experiment it is useful to focus on reactive powers. From Fig. 15d (and Fig. 16b), it can be seen that the third set transfers some reactive power (4.2%, or 11 VAr, of total simulated, 5.6%, or 15 VAr, of total measured) while its sharing coefficient for the field-producing current (k_{d3}) is zero - Fig. 15c (and Fig. 16a), sector **3**. This verifies that the sets do not transfer power between themselves exactly according to the torque-sharing coefficients.

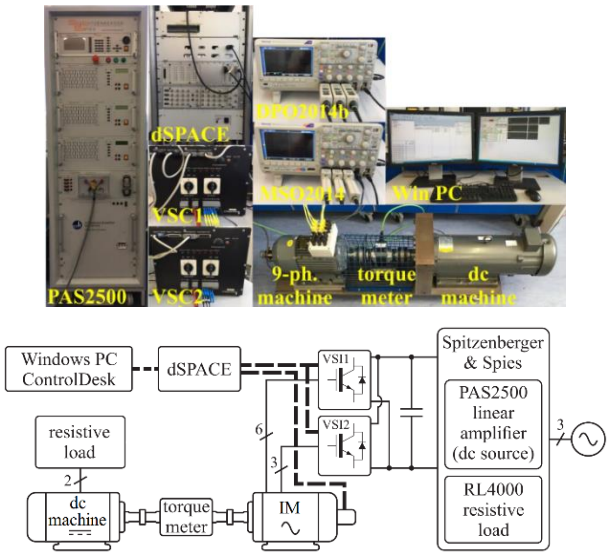

Fig. 14. Experimental rig and its electrical scheme.

TABLE I
TORQUE SHARING AND POWER SHARING COEFFICIENTS

Torque sharing					Power sharing				
sector	**1**	**2**	**3**	**4**	sector	**5**	**6**	**7**	**8**
time [s]	0-0.2	0.2-0.4	0.4-0.8	0.8-1	time [s]	1-1.2	1.2-1.6	1.6-1.8	1.8-2
k_{q1}	1/3	1/2	1/2	1/2	$k_{q'1}$	1/2	1/2	1/2	1/3
k_{q2}	1/3	0	0	0	$k_{q'2}$	0	0	0	1/3
k_{q3}	1/3	1/2	1/2	1/2	$k_{q'3}$	1/2	1/2	1/2	1/3
k_{d1}	1/3	1/2	1	1/2	$k_{d'1}$	1/2	1	1/2	1/3
k_{d2}	1/3	0	0	0	$k_{d'2}$	0	0	0	1/3
k_{d3}	1/3	1/2	0	1/2	$k_{d'3}$	1/2	0	1/2	1/3

B. *Power Sharing*

In order to allow a fair comparison, the power sharing mode is tested immediately after the torque sharing mode. Active and reactive power sharing coefficients are given in the right-hand part of Table I (1-2s). Their reference values are the same as those that were used in the previous sub-section for the torque sharing (although applied in the reverse order). The experimental results are given in the right-hand part of Fig. 15 (1-2s, sections **5**-**8**) and simulation results in the right-hand part of Fig. 16.

From Fig. 15d (and Fig. 16b), sector **6**, it can be seen that the transferred reactive power of the third set is nearly zero (0 % simulated, -0.4% measured) when its reference for reactive power is zero (Table I). This clearly validates the theoretical considerations from Section III-*B* and the proposed control from Section V-*B*.

Outputs of the "coef. correction" block (Fig. 11 and Fig. 13) are shown in Fig. 15c (and Fig. 16a - simulation). Clearly, they have different values from reactive power-sharing coefficients from the left part of the figures (0-1s, sectors **1**-**4**). This again demonstrates that the sets do not share power in the same way they share torque.

C. *Minimization of Additional Stator Winding Losses*

Finally, the control for minimization of stator copper losses (Section V-*C*) is tested. References for power sharing coefficients are given in Table II.

Two cases are compared. In one, reactive-power sharing coefficients are set to be equal to active-power sharing coefficients [15]. In the other, they are obtained from (21). In both cases, the machine spins at 1000 rpm at a load of 2 Nm. In addition, in both cases, the sets transfer the same amount of active power between themselves. Therefore, the only difference is in the reactive power that is sent between the sets.

TABLE II
POWER SHARING COEFFICIENTS, UTILIZED FOR LOSS COMPARISON

	Method according to [15]				Proposed method			
sector	**1**	**2**	**3**	**4**	**5**	**6**	**7**	**8**
time [s]	0-0.4	0.4-0.8	0.8-1.6	1.6-2	2-2.4	2.4-2.8	2.8-3.6	3.6-4
$k_{q'1}$	1	1/2	1	2/3	1	1/2	1	2/3
$k_{q'2}$	0	1/2	1	2/3	0	1/2	1	2/3
$k_{q'3}$	0	0	-1	-1/3	0	0	-1	-1/3
$k_{d'1}$	1	1/2	1	2/3	1/3	1/3	1/3	1/3
$k_{d'2}$	0	1/2	1	2/3	1/3	1/3	1/3	1/3
$k_{d'3}$	0	0	-1	-1/3	1/3	1/3	1/3	1/3

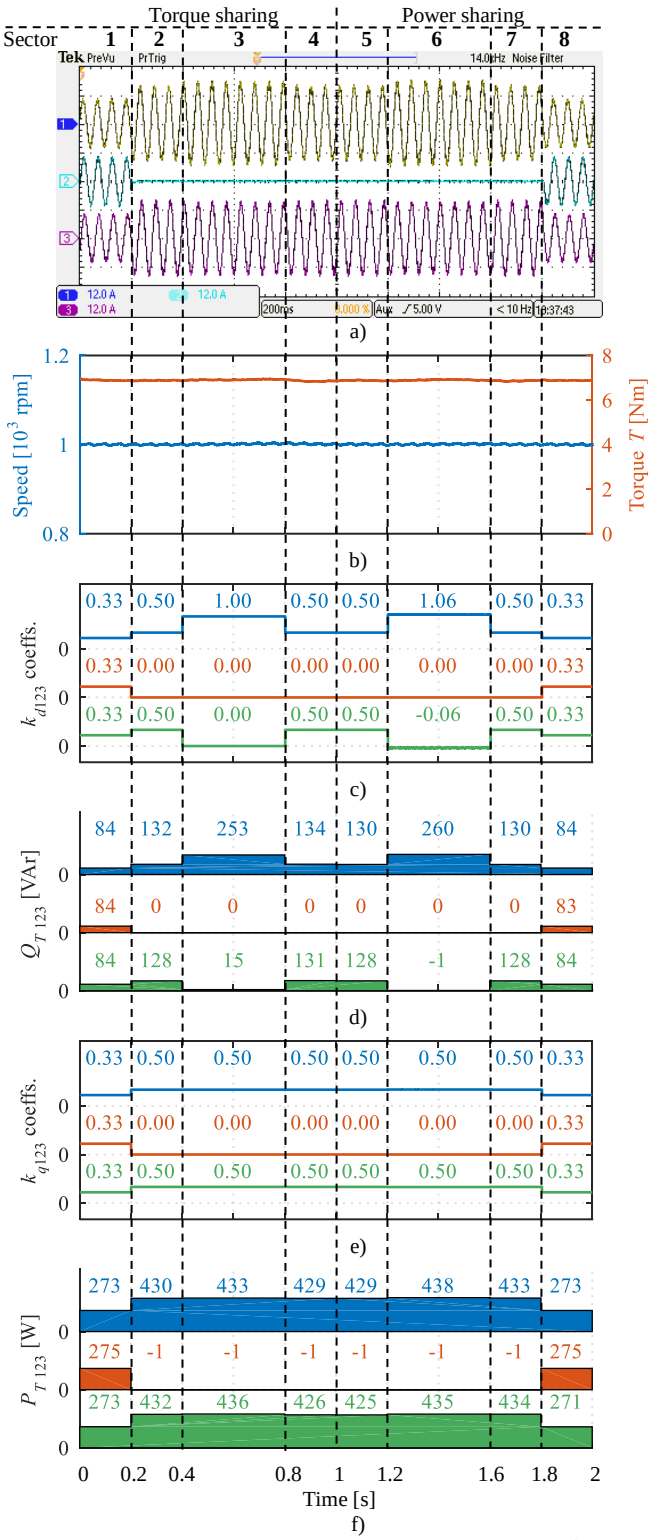

Fig. 15. Experimental comparison between torque sharing (left part) and power sharing (right-hand part) mode. a) Oscilloscope screenshot showing phase *a* current of each set (4 turns of the same wire enter each current probe in order to increase accuracy), b) IM speed and torque, c) coefficients for *d*-axis current of each set, d) transferred reactive power Q_{Tn} of each set (obtained at the end of each sector), e) coefficients for *q*-axis current of each set, f) transferred active power P_{Tn} of each set (obtained at the end of each sector).

The comparison results are given in Fig. 17. From Fig. 17f, a superiority of the here developed method is obvious. This validates theoretical considerations from Section III-*C*.

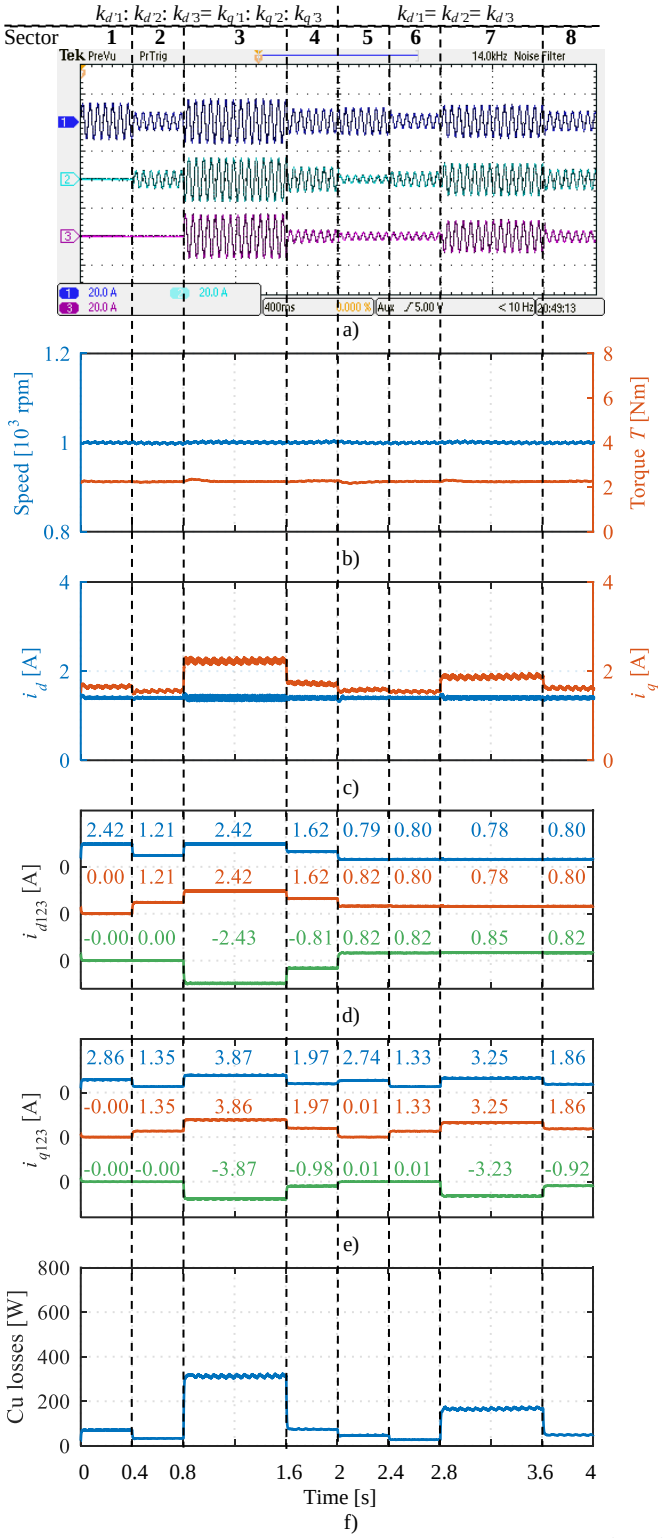

Fig. 17. Experimental comparison between two modes. In one (left half), reactive power coefficients match active power coefficients. In the other (right half), reactive power coefficients are always equal to each other (Section III-*C*). a) Oscilloscope screenshot showing phase *a* current of each set (4 turns of the same wire enter each current probe in order to increase accuracy), b) IM speed and torque, c) current *d*- and *q*-component, d) individual *d*-current component of each set, e) individual *q*-current component of each set, f) stator copper losses.

At last, it is useful to observe Fig. 17c, and particularly sectors **3** and **7**. This is the extreme case in which all the sets have the same power (P_{Tn}), but two sets are producing it and

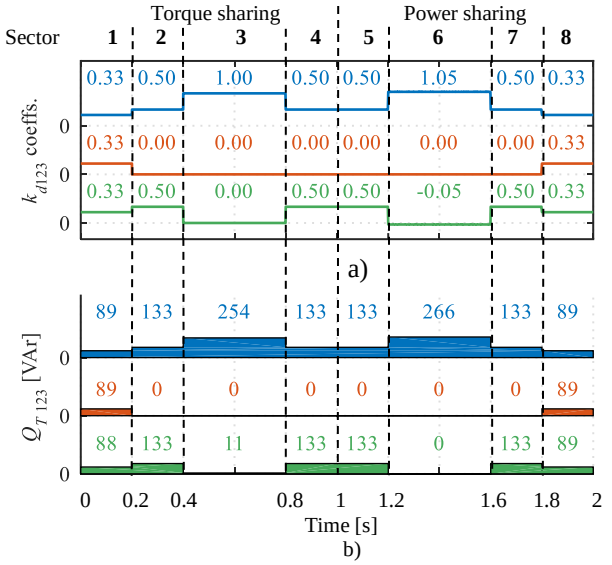

Fig. 16. Simulation comparison between torque sharing (left part) and power sharing (right-hand part). The conditions are the same as for Fig. 15. The figure shows: a) coefficients for *d*-axis current of each set and b) transferred reactive power Q_{Tn} of each set (obtained at the end of each sector). Machine torque and speed (not shown here) do not have variations in time and are equal to 7 Nm and 1000 rpm, respectively.

one is consuming it (Table II). Now, higher *q*-current is required in order to produce the same amount of torque. This is a direct consequence of the fact that a lower number of stator slots is utilized for producing power. As a result, spatial harmonics are produced, which degrade IM performances.

Quantification of these harmonics highly depends on machine design. Their analysis is out of the scope of this paper and will be a focus of future research. Nevertheless, a comparison between sectors **3** and **7** reveals that the undesired effect is significantly lower in the proposed method (sector **7**).

VII. Conclusion

This paper introduces a method for accurate active and reactive power transfer between sets of windings of a multiphase induction machine. It provides a clear demonstration that the sets do not share the power in the same manner as they share the torque. Finally, it proposes a method for minimization of stator copper losses. Theoretical results and the control scheme, developed in the paper, are validated by simulations and experiments.

VIII. Appendix

Dc source: "Spitzenberger & Spies" – two DM 2500/ PAS mains emulation systems are connected in series.

Controller: dSPACE DS1006 processor board. DS2004 high-speed A/D board is used for the A/D conversion of the measured machine currents. DS5101 Digital Waveform Output Board is used for the PWM and the machine speed is read by a DS3002 incremental encoder interface board.

Converters: Two two-level eight-phase inverters with EUPEC FS50R12KE3 IGBTs. Each has a continuous rating of approximately 28 kVA.

Asymmetrical nine-phase induction machine: 2.2 kW, 220 V (phase-to-neutral), 1.5 A, 50 Hz, one pole pair, R_s = 5 Ω,

R_r = 2.6 Ω, L_{ys} = 19 mH, L_{yr} = 9 mH, and L_m = 1.1 H.
Dc machine: Baldor, 180 V, 3.7 kW, 1750 r/min.
Torque meter: Magtrol TM 210.

REFERENCES

[1] S. Parhizi, H. Lotfi, A. Khodaei and S. Bahramirad, "State of the art in research on microgrids: a review," *IEEE Access*, vol. 3, pp. 890-925, 2015.

[2] H. Han, X. Hou, J. Yang, J. Wu, M. Su and J. M. Guerrero, "Review of power sharing control strategies for islanding operation of AC microgrids," *IEEE Trans. Smart Grid*, vol. 7, no. 1, pp. 200-215, 2016.

[3] T. Dragičević, X. Lu, J. C. Vasquez and J. M. Guerrero, "DC microgrids—part II: a review of power architectures, applications, and standardization issues," *IEEE Trans. Power Elect.*, vol. 31, no. 5, pp. 3528-3549, 2016.

[4] A. Khaligh and Z. Li, "Battery, ultracapacitor, fuel cell, and hybrid energy storage systems for electric, hybrid electric, fuel cell, and plug-in hybrid electric vehicles: state of the art," *IEEE Trans. Vehicular Tech.*, vol. 59, no. 6, pp. 2806-2814, 2010.

[5] S. Hu, Z. Liang, W. Zhang and X. He, "Research on the integration of hybrid energy storage system and dual three-phase PMSM drive in EV," *IEEE Trans. Ind. Elect.*, vol. 65, no. 8, pp. 6602-6611, 2018.

[6] A. Galassini, A. Costabeber, C. Gerada and A. Tessarolo, "Distributed speed control for multi-three phase electrical motors with improved power sharing capability," in *Proc. IEEE Energy Conv. Congress and Expo. (ECCE)*, Cincinnati, OH, pp. 2492-2497, 2017.

[7] A. Galassini, A. Costabeber, C. Gerada, A. Tessarolo and R. Menis, "Speed control with load sharing capabilities for multi-three phase synchronous motors," in *Proc. IEEE Ind. Elect. Society Conf. (IECON)*, Beijing, China, pp. 4408-4413, 2017.

[8] F. Luise, S. Pieri, M. Mezzarobba, and A. Tessarolo, "Regenerative testing of a concentrated-winding permanent-magnet synchronous machine for offshore wind generation – Part I: Test concept and analysis," *IEEE Trans. Ind. Appl.*, vol. 48, no. 6, pp. 1779-1790, 2012.

[9] F. Luise, S. Pieri, M. Mezzarobba, and A. Tessarolo, "Regenerative testing of a concentrated-winding permanent-magnet synchronous machine for offshore wind generation – Part II: Test implementation and results," *IEEE Trans. Ind. Appl.*, vol. 48, no. 6, pp. 1791-1796, 2012.

[10] M. Zabaleta, E. Levi and M. Jones, "A novel synthetic loading method for multiple three-phase winding electric machines," *IEEE Trans. Energy Conv.*, vol. 34, 2019 (accepted for publication).

[11] G. Scarcella, G. Scelba, M. Cacciato, A. Spampinato and M. M. Harbaugh, "Vector control strategy for multidirectional power flow in integrated multidrives starter-alternator applications," *IEEE Trans. Ind. Appl.*, vol. 52, no. 6, pp. 4816-4826, 2016.

[12] M. J. Duran, I. González-Prieto, A. González-Prieto and F. Barrero, "Multiphase energy conversion systems connected to microgrids with unequal power-sharing capability," *IEEE Trans. Energy Conv.*, vol. 32, no. 4, pp. 1386-1395, 2017.

[13] R. Bojoi, A. Tenconi, F. Profumo and F. Farina, "Dual-source fed multi-phase induction motor drive for fuel cell vehicles: topology and control," in *Proc IEEE Power Elect. Specialists Conf. (PESC)*, Recife, Brazil, pp. 2676-2683, 2005.

[14] H. S. Che, E. Levi, M. Jones, M. J. Duran, W. P. Hew and N. A. Rahim, "Operation of a six-phase induction machine using series-connected machine-side converters," *IEEE Trans. Ind. Elect.*, vol. 61, no. 1, pp. 164-176, 2014.

[15] I. Zoric, M. Jones and E. Levi, "Arbitrary power sharing among three-phase winding sets of multiphase machines," *IEEE Trans. Ind. Elect.*, vol. 65, no. 2, pp. 1128-1139, 2018.

[16] M. Mengoni, G. Sala, L. Zarri, A. Tani, G. Serra, Y. Gritli, and M. Duran, "Control of a fault-tolerant quadruple three-phase induction machine for more electric aircrafts," in *Proc IEEE Ind. Elect. Society Conf. (IECON)*, Florence, Italy, pp. 5747-5753, 2016.

[17] S. Rubino, R. Bojoi, A. Cavagnino and S. Vaschetto, "Asymmetrical twelve-phase induction starter/generator for more electric engine in aircraft," in *Proc. IEEE Energy Conv. Congress and Expo. (ECCE)*, Milwaukee, WI, pp. 1-8, 2016.

[18] A. Tani, G. Serra, M. Mengoni, L. Zarri, G. Rini and D. Casadei, "Dynamic stator current sharing in quadruple three-phase induction motor drives," in *Proc IEEE Ind. Elect. Society Conf. (IECON)*, Vienna, Austria, pp. 5173-5178, 2013.

[19] R. H. Nelson and P. C. Krause, "Induction machine analysis for arbitrary displacement between multiple winding sets," *IEEE Trans. Power App. and Syst.*, vol. PAS-93, no. 3, pp. 841-848, 1974.

[20] E. Levi, R. Bojoi, F. Profumo, H. A. Toliyat and S. Williamson, "Multiphase induction motor drives - a technology status review," *IET Electr. Power Applicat.*, vol. 1, no. 4, pp. 489-516, 2007.

[21] D. Dujic, E. Levi and M. Jones, "Dc bus utilisation in multiphase VSI supplied drives with a composite stator phase number," in *Proc. IEEE Int. Conf. on Ind. Technology (ICIT)*, Vina del Mar, Chile, pp. 1495-1500, 2010.

Ivan Subotic (S'12, M'16) received the Dipl. Ing. and MSc degrees in Electrical Engineering from the University of Belgrade, Belgrade, Serbia, in 2010 and 2011, respectively. He has been with the Liverpool John Moores University, Liverpool, U.K., as a PhD student since 2011. He received his PhD degree in September 2015 and then joined ETH Zurich, as a post-doctoral research associate. In 2017 he returned to Liverpool John Moores University as a post-doctoral research associate. His main research interests include power electronics, electric vehicles, and control of multiphase drive systems.

Obrad Dordevic (S'11, M'13) received his Dipl. Ing. degree in Electronic Engineering from the University of Belgrade, Serbia, in 2008. He joined Liverpool John Moores University in December 2009 as a PhD student. Dr Dordevic received his PhD degree in April 2013 and was appointed a Lecturer at the Liverpool John Moores University in May 2013. In 2018 he was promoted to a Reader in Power Electronics. His main research interests are in the areas of power electronics, electrostatic precipitators, and advanced variable speed multiphase drive systems.

Barry Gomm (M'92) received the BEng (Hons) degree in Electrical and Electronic Engineering in 1987 and PhD degree in Control Engineering in 1991 from Liverpool Polytechnic, UK. He joined Liverpool John Moores University, UK in 1991 and is a Reader in Intelligent Control Systems since 2000. His main research interests include neural networks for modelling, control and fault diagnosis of non-linear processes, intelligent methods for control, system identification and adaptive systems.

Emil Levi (S'89, M'92, SM'99, F'09) received his MSc and the PhD degrees in Electrical Engineering from the University of Belgrade, Yugoslavia in 1986 and 1990, respectively. He joined Liverpool John Moores University, UK in May 1992 and is since September 2000 Professor of Electric Machines and Drives. He served as a Co-Editor-in-Chief of the IEEE Trans. on Industrial Electronics in the 2009-2013 period. Currently he is Editor-in-Chief of the IEEE Trans. on Industrial Electronics, Editor-in-Chief of the IET Electric Power Applications and an Editor of the IEEE Trans. on Energy Conversion. He is the recipient of the Cyril Veinott award of the IEEE Power and Energy Society for 2009 and the Best Paper award of the IEEE Trans. on Industrial Electronics for 2008. In 2014 he received the "Outstanding Achievement Award" from the European Power Electronics (EPE) Association and in 2018 the "Professor Istvan Nagy Award" from the Power Electronics and Motion Control (PEMC) Council.